Immunomagnetic Enrichment and Flow Cytometric Characterization of Mouse Microglia

Supinder S. Bedi[1,*], **Philippa Smith**[1,*], **Robert A. Hetz**[1,2], **Hasen Xue**[1], and **Charles S. Cox**[1,2,3]

[1]Department of Pediatric Surgery, University of Texas, Health Science Center at Houston, Houston, Texas

[2]Department of Surgery, University of Texas, Health Science Center at Houston, Houston, Texas

[3]Michael E DeBakey Institute for Comparative Cardiovascular Science and Biomedical Devices, Texas A & M University, College Station, Texas

Abstract

Background—The inflammatory response after a CNS injury is regulated by microglia/macrophages. Changes in the ratio of M1 classically activated pro-inflammatory cells versus M2 alternatively activated anti-inflammatory cells reveal the direction of the immune response. These cells are routinely identified and enumerated by morphology and cell-surface markers using immunohistochemistry.

New Method—We used a controlled cortical impact (CCI) mouse model for traumatic brain injury (TBI), then isolated microglia/macrophages from neural cell suspensions using magnetic beads conjugated to CD11b monoclonal antibody to obtain the entire myeloid population. Polarization states of $CD11b^+CD45^{lo}$ microglia were evaluated by expression of M1 surface marker F_c RII/III and M2 surface marker CD206.

Results—After TBI, we observed an increase in M1:M2 ratio in the ipsilateral hemisphere when compared to the contralateral side, indicating that 24 hours after CCI, a shift in microglia polarization occurs localized to the hemisphere of injury.

Comparison with Existing Method(s)—The major impetus for developing and refining the methods was the need to accurately quantify microglial activation states without reliance on manual morphometric counting of serial immunohistochemistry slides. Flow cytometric analysis of enriched cell suspensions provides quantitative measurement of microglial polarization states complementary to existing methods, but for entire populations of cells.

Conclusions—In summary, we used immunomagnetic beads to isolate myeloid cells from injured brain, then stained surface antigens to flow cytometrically identify and categorize microglia as either classically activated M1 or alternatively activated M2, generating a ratio of M1:M2 cells which is useful in studying attempts to reduce or redirect neuroinflammation.

Address inquiries to: Charles S. Cox Jr., MD, Department of Pediatric Surgery, University of Texas, Health Science Center at Houston, 6431 Fannin Street, MSB 5.236, Houston, Texas, 77030, Phone: (713) 500-7300, Fax: (713) 500-7296, Charles.S.Cox@uth.tmc.edu.
*Equal contribution

MeSH Keywords

Traumatic brain injury; microglia; neuroinflammation; flow cytometry

Introduction

The central nervous system (CNS) is a complex arrangement of interacting cells of two types: glia and neurons. Microglia, CNS resident immune cells of the myeloid lineage, constitute approximately 5–10% of the brain's glial cells (Nakajima and Kohsaka, 2001). CNS injuries, including traumatic brain injury (TBI), are characterized by disruption of the blood brain barrier (BBB), subsequent influx of infiltrating macrophages (Pineau et al., 2010), and release of pro-inflammatory cytokines such as interleukin-1 and tumor necrosis factor (Pineau and Lacroix, 2007) which activate microglia via their surface receptors (Gordon, 2003). After injury, it is difficult to distinguish between activated CNS microglia/ macrophages and infiltrating macrophages, since the two cell types have similar morphologies and antigen presenting capabilities (Streit, 2002).

Microglia can be classified as either M1 or M2 based on morphology and/or cell surface antigens (Ransohoff and Perry, 2009). Microglia, in the presence of anti-inflammatory cytokines such as interleukin-4 (IL-4) and interleukin-10 (IL-10) are generally in a resting/ ramified/surveillant state known as M2, or alternatively activated (Nimmerjahn et al., 2005, Graeber, 2010). M2 microglia have small, static cell bodies with dynamic, branched processes and express the macrophage mannose receptor 1 (MMR, or CD206) on the cell membrane and Arginase-1, the prototypical M2 marker, intracellularly. Lipopolysaccharide and interferon- promote the differentiation of M1 microglia/macrophages, which have a distinct amoeboid morphology and are generally phagocytic (Smith, 2010). Markers such as CD86, iNOS, MHCII, and CD16/32 have been used to identify M1-polarized cells (David and Kroner, 2011). Following a CNS injury, the immune response is regulated by microglia/ macrophages (Kigerl et al., 2009), thus changes in the ratio of M1 to M2 cells suggest the direction and progress of this response. The peaks of the pro-inflammatory mediators are within the first 24 hours after injury, followed by anti-inflammatory cytokines (IL-4 and IL-10) for 96 hours (Loane and Byrnes, 2010). Immediately after injury the M1:M2 ratio is typically 1:1, but the ratio becomes M1-predominate as the response develops on days 3–7 after injury (Walker et al, 2012).

Microglia are routinely enumerated and classified by morphology and cell-surface markers using immunohistochemistry (Bedi et al, In press). The major impetus for developing and refining the methods presented here was the need to accurately quantify microglial activation states in entire populations of cells from large regions and/or entire brains without reliance on manual morphometric counting of serial immunohistochemistry slides. We used immunomagnetic bead separation/enrichment followed by four-color flow cytometric analysis of fluorescently labeled surface markers on microglia to enumerate the M1 and M2 populations from ipsilateral and contralateral brain hemispheres twenty-four hours after TBI.

Material and Methods

Adult male C57B6 mice (Harlan, Indianapolis, IN, USA) were housed on a 12-hour light/ dark cycle with ad libitum access to food and water. All protocols involving the use of animals were in compliance with the National Institutes of Health Guide for the Care and Use of Laboratory Animals and were approved by the Institutional Animal Care and Use Committee (HSC-AWC-11-023).

Injury

A controlled cortical impact (CCI) device (Impact One Stereotaxic Impactor, Leica Microsystems, Buffalo Grove, IL) was used to administer a unilateral brain injury to six to eight week old normal adult male C57B6 mice weighing 17–21 grams. Mice were anesthetized with 4% isoflurane/O_2 and the head mounted in a stereotactic frame. Animals received a single impact to the right parietal association cortex of 1.0-mm depth of deformation with an impact velocity of 5.0 m/sec and a dwell time of 200 milliseconds (moderate-severe injury). After the injury, the incision was closed with staples.

Isolation of Microglia

24 hours after injury, mice were anesthetized with 4% isoflurane/O_2, sacrificed via right atrial puncture, and perfused with PBS. Brains were excised and the cerebellum removed; in injured animals the hemispheres were divided for separate processing (Fig. 1). Microglia were isolated from brain tissue by enzymatic digestion and mechanical dissociation followed by myelin removal and immunomagnetic cell separation (Neural Dissociation Kit, gentleMax Dissociator, MACSMix, Myelin Removal Beads II, and CD11b Microbeads, Miltenyi Biotech, Cambridge, MA). Manufacturer's protocols were followed with the exception of increases in single runs of gentleMax mouse brain program #1 to three runs and #2 to two runs, to ensure complete tissue dissociation. Program #3 was run only once, as directed.

Flow Cytometry

Unseparated, negative (effluent), and CD11b-enriched cell populations were surface-stained with F_c RII/III (CD16/32) PerCP-Cy5.5 (BD Biosciences, San Jose, CA), CD45 APC-Cy7, CD11b-biotin, and CD206 APC (BioLegend, San Diego, CA) for 15 minutes at 4°C, washed and resuspended for a secondary 15 minute incubation at 4°C with streptavidin-PE (BioLegend, San Diego, CA), then washed and resuspended once more before data acquisition. All incubations and washes were done in freshly filtered AutoMACS running buffer (Miltenyi Biotech, Cambridge, MA).

Data was acquired with an LSRII cytometer (BD Biosciences, San Jose, CA) and analyzed with FlowJo (TreeStar, Ashland, OR). Fluorescence spillover compensation values were generated using pooled unseparated/enriched cell preparations rather than commercially available beads to account for the high autofluorescence of myeloid cells. Debris and aggregates were eliminated from the analysis by forward and side scatter characteristics, then myeloid cells identified as CD11b$^+$ singlets (Fig. 2A) were divided into CD45^{lo} microglia and a small CD45^{hi} subpopulation (Fig. 3A). Polarization states of CD11b$^+$CD45^{lo} microglia were evaluated by expression of M1 marker F_c RII/III and M2 marker CD206 (Fig. 4A) with gates established by fluorescence minus one (FMO) controls. For each brain or hemisphere, approximately ten thousand CD11b$^+$ singlets were analyzed.

Statistical Analysis

Unless otherwise indicated, all values are represented as mean ± SEM. Values for ipsilateral and contralateral hemispheres were compared using Paired T-test. We used the Unpaired T-test to compare between Sham and ipsilateral CCI. A p value of 0.05 was used to denote statistical significance. * indicates $p < 0.05$, ** indicates $p < 0.01$, and *** indicates $p < 0.005$. A one-tailed p value of 0.05 was denoted by #.

Results

Altered frequencies of both myeloid and nonmyeloid leukocytes in brain 24 hours after CCI

Although not directly related to our primary goal here to establish an efficient flow cytometric method for assessing global microglial polarization states after TBI, our analysis revealed significant differences in frequencies of both myeloid and nonmyeloid leukocyte populations after CCI. Twenty-four hours after injury, unseparated neural cell suspensions from injured ipsilateral CCI-R hemispheres contained $5.1\% \pm 1.8$ $CD11b^+$ cells (Fig. 2A red box and Fig. 2B), a significantly lower percentage than that found in contralateral CCI-L hemispheres ($14.8\% \pm 3.9$, $p < 0.005$) and in uninjured brains ($12.3\% \pm 5.3$, $p < 0.01$). Additionally, the small but measurable fraction of $CD11b^-CD45^+$ nonmyeloid leukocytes present (Fig. 2A blue box and Fig. 2C) was significantly higher ($p < 0.05$) in CCI-L ($4.1\% \pm 1.5$) than in CCI-R hemispheres ($2.5\% \pm 1.4$), which were similar to uninjured brains ($2.6\% \pm 0.2$). Thus, considerable changes in the composition of the immune compartment relative to uninjured brains are evident twenty-four hours after TBI both ipsilateral (reduced myeloid leukocyte percentage) and contralateral (increased nonmyeloid leukocyte percentage) to the injury.

Purity (Fig. 2D) and enrichment efficiency (Fig. 2E) of myeloid cell suspensions varied with experimental conditions, but in all cases yields were sufficient for flow cytometric analysis and viability >90% (Trypan Blue exclusion, data not shown). While the reduced numbers of $CD11b^+$ cells present in ipsilateral CCI-R hemispheres were enriched >10-fold (Fig. 2E), resulting suspensions reached only $48\% \pm 11$ purity (Fig. 2D). The relatively greater numbers of myeloid cells present in uninjured brains and contralateral CCI-L hemispheres were typically enriched 5- to 7-fold (Fig. 2E) and achieved a significantly greater purity (Fig. 2D, $73\% \pm 4.6$ and $71\% \pm 3.6$, respectively) in comparison to ipsilateral CCI-R hemispheres ($p < 0.01$). Negative (effluent) fractions showed very few $CD11b^+$ cells present (data not shown).

Small $CD45^{hi}$ myeloid population increased 24 hours after CCI

We observed a small population of $CD11b^+CD45^{hi}$ cells in all brains and hemispheres (Fig. 3A, blue box). These cells displayed higher forward scatter (an optical parameter based on refractive index and associated with cell size) values and brighter CD11b and F_c RII/III staining (Fig. 3B, blue lines) than the $CD45^{lo}$ microglial population (red box, red lines), suggesting the $CD45^{hi}$ cells are larger and express surface activation markers at higher levels than $CD45^{lo}$ microglia. $CD11b^+CD45^{hi}$ cells have been noted and described as endogenous CNS macrophages in a noninflammatory context (Ford et al., 1995) and as either infiltrating macrophages (Jin et al., 2012) or a combination of infiltrating neutrophils and monocyte/macrophages (Stirling and Yong, 2008) in CNS injury scenarios. In injured brains, $CD11b^+CD45^{hi}$ cells are likely a mixed population of inflammatory myeloid cell types (neutrophils, infiltrating monocyte/macrophages, activated CNS microglia/macrophages, and possibly a few dendritic cells), the composition of which varies as the immune response develops. Twenty-four hours after injury, the frequency of these cells increased significantly (Fig. 3C) in ipsilateral CCI-R ($8.3\% \pm 1.6$) versus contralateral CCI-L hemispheres ($4.2\% \pm 0.6$, $p < 0.05$), while complementary changes in frequency of the majority $CD11b^+CD45^{lo}$ microglial population (Fig. 3D) were also noted ($91\% \pm 1.6$ in CCI-R versus $95\% \pm 1$ in CCI-L, $p < 0.05$). Differences between CCI-R and uninjured brains did not reach significance, since considerable variation in $CD11b^+CD45^{hi}$ cell frequency appears to exist in brains of normal mice.

Microglial M1:M2 ratio increased 24 hours after CCI

While macrophage polarization is a dynamic process which generates complex overlapping patterns of surface marker expression among multiple subtypes of cells (David and Kroner, 2011), a simple binary categorization of $CD11b^+CD45^{lo}$ microglia based on expression of macrophage mannose receptor 1 (MMR, CD206) and low affinity F_c receptors IIB and III (F_c RII/III, CD16/32) served to reveal significant changes in microglial polarization states twenty-four hours after CCI. As expected, the majority of microglia in all instances were F_c RII/III$^+$ and were subdivided into CD206$^-$ M1 cells (Fig 4A, red box) and CD206$^+$ M2 cells (Fig 4A, blue box). Twenty-four hours after injury, the frequency of M1 cells as a percentage of all microglia increased to $76 \pm 2.0\%$ in ipsilateral CCI-R versus $70 \pm 3.8\%$ in contralateral CCI-L hemispheres (Fig. 4B, $p = 0.0565$) while the frequency of M2 cells decreased to $9.4 \pm 0.7\%$ in CCI-R from $12 \pm 0.8\%$ in CCI-L hemispheres (Fig. 4C, $p < 0.05$). This slight increase in M1 frequency combined with the substantial decrease in M2 frequency generated a significant rise in the microglial M1:M2 ratio (Fig. 4D) in ipsilateral CCI-R (8.3 ± 0.5) versus contralateral CCI-L (6.0 ± 0.6, $p < 0.05$) hemispheres and uninjured brains (6.1 ± 1.2, $p < 0.05$) at this timepoint.

Discussion

In this study, we describe the use of flow cytometric methods to evaluate the global polarization state of the entire microglial population in immunomagnetically enriched brain cell suspensions in a mouse model of TBI (Fig. 1). Using monoclonal antibodies against surface antigens to identify microglia and characterize their polarization state, we found a significant increase in the ratio of classically activated M1 versus alternatively activated M2 microglia in ipsilateral brain hemispheres twenty-four hours after TBI (Fig. 4D). This change in M1:M2 ratio was produced by a significant decrease in frequency of anti-inflammatory M2 cells (Fig. 4C). These data are important because microglial activation state is an emerging therapeutic target for anti-inflammatory strategies in neurological injuries and diseases. Reproducible, quantitative measurement of whole brains and regions of interest allows development of therapies targeting this aspect of the neuroinflammatory response. Additional analysis of data collected to assess enrichment efficiency demonstrated additional significant global changes in both the frequencies and characteristics of myeloid and nonmyeloid leukocyte subpopulations in the brain at this time point (Figs. 2, 3).

A 1990 study (Loane and Byrnes, 2010) found that microglia (as determined by F4/80 staining of brain slices) are distributed irregularly in the normal mouse brain and constitute 5 to 12% of total brain cells in various sections. While immunohistochemical methods are indispensable for evaluating intact CNS cell morphologies and can at times make semiquantitative morphometry possible and subcellular localization achievable (Ransohoff and Perry, 2009), they are also notoriously prone to artifact, which can be hard to detect, and require preparation of fixed tissue and extensive manual counting of cells. The use of complementary flow cytometric techniques in parallel to immunohistochemistry allows more accurate enumeration and characterization of whole populations of cells from entire brains or hemispheres, not just localized regions. An additional advantage to incorporating flow cytometry is the ability to design multicolor antibody panels to delineate subpopulations in ways not possible using immunohistochemistry.

Flow cytometric analysis of total brain cell suspensions, while very useful for revealing overall dynamics of multiple immune cell types after injury (Stirling and Yong, 2008, Jin et al., 2012), requires large amounts of antibodies to stain relatively rare cells, which then comprise only a small fraction of the collected and stored data. Therefore, enrichment of the total unseparated neural cell suspension for the cell type of interest is desirable when characterization of a single subpopulation is the goal rather than determining the relative

frequencies of various cell types. Similar immunomagnetic separation methods have recently been shown to efficiently enrich, but importantly do not activate, mouse microglia (Nikodemova and Watters, 2012). Flow cytometry overcomes the two- or three-color limitations of immunohistochemistry techniques, e.g. allowing for better characterization of cells by simultaneous measurement of M1 and M2 markers in addition to both the   integrin CD11b and the leukocyte common antigen CD45 to distinguish microglia from other myeloid cell types.

While the primary component of enriched cell suspensions was the $CD11b^+CD45^{lo}$ microglia we sought to characterize, a small $CD11b^+CD45^{hi}$ population was also evident and increased significantly in injured brain hemispheres (Fig. 3C). The identity of these relatively rare $CD11b^+CD45^{hi}$ cells seems to vary with the physiological context and in our case is likely a mixed population of neutrophils and macrophages. Initial experiments in rat brains showed that in the absence of injury or inflammation, this population consists of endogenous CNS macrophages, not blood-derived infiltrating cells (Ford et al., 1995). Later work done using flow cytometry in a mouse spinal cord injury model used the Gr-1 antibody to discriminate neutrophils from microglia/macrophages and found the $CD11b^+CD45^{hi}$ population in injured cords to be mostly neutrophils with a few monocytes up to 48 hours after injury (Stirling and Yong, 2008). A more recent flow cytometric study in a mouse model of TBI (Jin et al., 2012) describes all $CD11b^+CD45^{hi}$ cells as macrophages, leaving some doubt as to whether neutrophils were eliminated from this population before analysis. A neutrophil marker such as Gr-1 could easily be added to our four-color panel to enable M1/M2 ratio analysis of rare $CD11b^+CD45^{hi}Gr-1^{neg}$ microglia/macrophages in addition to the $CD11b^+CD45^{lo}$ microglia described in Figure 4. These $CD11b^+CD45^{hi}Gr-1^{neg}$ cells cannot be considered exclusively blood-derived until a method to discriminate between infiltrating blood monocytes/macrophages and resident CNS microglia/macrophages is developed.

We avoided the use of intracellular staining here because permeabilization conditions have been shown to critically affect results in both B cells (Verdier et al., 2000) and T cells (Papagno et al., 2007), suggesting that optimization of intracellular flow cytometry protocols for microglia/macrophages will not be trivial. Additional benefits of limiting the protocol to surface stains are the retained ability to sort live cells for functional experiments, as well as a significant reduction in time and labor. We chose surface antigens CD206 and Fc RII/III (CD16/32) to examine M1:M2 ratios ipsilateral and contralateral to the injury. CD206, macrophage mannose receptor 1, is perhaps the prototypical anti-inflammatory surface marker and has been used to identify M2 microglia in TBI and SCI (Kigerl et al., 2009, Walker et al., 2012) as well as in studies of macrophage polarization in other tissues. Our group has previously used T-cell coreceptor ligand CD86 as an M1 marker, but after cultured microglia seemed to lose CD86 expression (possibly due to enzymatic cleavage upon removal from growth surfaces) we became concerned about the need to use the same staining panel in both in vivo and ex vivo microglia experiments and chose CD16/32 as a substitute. Both low affinity activating (Fc RIII, CD16) and inhibitory (Fc RIIB, CD32) Fc receptors bind immune complexes composed of IgG antibodies bound to soluble antigens from invading pathogens, infected cells, or necrotic and apoptotic debris, and are intimately involved in regulation of important aspects of immune responses such as activation of innate effector cells, antigen presentation, dendritic cell maturation, and B cell activation and plasma cell survival (Nimmerjahn and Ravetch, 2008). While the functional significance of expression of the various Fc Rs on microglia remains to be illuminated, CD16/32 reagents are used as M1 markers in the CNS (Guerrero et al., 2012), and the general capability of pro-inflammatory cytokines and mediators such as tumor necrosis factor, lipopolysaccharide, and interferon-   to upregulate expression of activating Fc Rs has been demonstrated and supports the role of these receptors in mediating antibody activity; the

inhibitory FcRIIB is able to induce endocytosis or phagocytosis after crosslinking (Nimmerjahn and Ravetch, 2008).

Consistent with a previous report describing similar methods (Nikodemova and Watters, 2012), we always found a bimodal distribution of microglia divergent in forward scatter (Figs 2, 3, 4 top right small plots, and Fig. 3B left plot red line), with FSC^{hi} cells generally brighter in all surface markers. The ratio of FSC[hi] to FSC^{lo} cells varied across experimental conditions, suggesting a higher occurrence of FSC[hi] microglia may be associated with inflammation (data not shown). However, there was considerable variability within each group, and the data did not reach significance. A potential relationship of forward scatter characteristics to microglial physiology remains to be elucidated.

Although we observed both a slight increase in %M1 and a significant decrease in %M2 microglia in injured hemispheres twenty-four hours after CCI, the change in the M1:M2 ratio is critical in determining whether the immune response is directed along a pro-inflammatory or an anti-inflammatory path, and M1:M2 ratios have been previously used in SCI and TBI to describe microglial polarization states (Walker, 2012). SCI results in an increase in M1 classically activated pro-inflammatory microglia at the site of injury (Kigerl et al., 2009). Time course studies using the methods described here to track M1:M2 ratios after injury and treatment should prove useful.

Conclusion

We analyzed microglia/macrophages in injured and uninjured mouse neural cell suspensions using magnetic beads conjugated to CD11b monoclonal antibody to obtain the entire myeloid population (Figs. 1 and 2), then identified microglia flow cytometrically as CD11b^{+}CD45^{lo} cells and evaluated their expression of M1 and M2 surface markers (Figs. 3 and 4). We observed an increase in microglial M1:M2 ratio in ipsilateral injured hemispheres compared to both contralateral hemispheres and uninjured brains (Fig. 4D), indicating that twenty-four hours after CCI, a shift in microglia polarization occurs localized to the hemisphere of injury. In summary, we used immunomagnetic beads to isolate the myeloid compartment from injured brain and stained surface antigens to identify microglia flow cytometrically and classify them as either classically activated pro inflammatory M1 or alternatively activated anti-inflammatory M2, generating a ratio of M1:M2 which is useful in studying attempts to reduce or redirect neuroinflammation.

Supplementary Material

Refer to Web version on PubMed Central for supplementary material.

Acknowledgments

References

David S, Kroner A. Repertoire of microglial and macrophage responses after spinal cord injury. Nat Rev Neurosci. 2011; 12:388–399. [PubMed: 21673720]

Ford AL, Goodsall AL, Hickey WF, et al. Normal adult ramified microglia separated from other central nervous system macrophages by flow cytometric sorting. Phenotypic differences defined and direct ex vivo antigen presentation to myelin basic protein-reactive CD4+ T cells compared. J Immunol. 1995; 154:4309–4321. [PubMed: 7722289]

Gordon S. Alternative activation of macrophages. Nat Rev Immunol. 2003; 3:23–35. [PubMed: 12511873]

Graeber MB. Changing face of microglia. Science. 2010; 330:783–788. [PubMed: 21051630]

Guerrero AR, Uchida K, Nakajima H, et al. Blockade of interleukin-6 signaling inhibits the classic pathway and promotes an alternative pathway of macrophage activation after spinal cord injury in mice. J Neuroinflammation. 2012; 9:40. [PubMed: 22369693]

Jin X, Ishii H, Bai Z, et al. Temporal changes in cell marker expression and cellular infiltration in a controlled cortical impact model in adult male C57BL/6 mice. PloS one. 2012; 7:e41892. [PubMed: 22911864]

Kigerl KA, Gensel JC, Ankeny DP, et al. Identification of two distinct macrophage subsets with divergent effects causing either neurotoxicity or regeneration in the injured mouse spinal cord. J Neurosci. 2009; 29:13435–13444. [PubMed: 19864556]

Loane DJ, Byrnes KR. Role of microglia in neurotrauma. Neurotherapeutics. 2010; 7:366–377. [PubMed: 20880501]

Nakajima K, Kohsaka S. Microglia: activation and their significance in the central nervous system. J Biochem. 2001; 130:169–175. [PubMed: 11481032]

Nikodemova M, Watters JJ. Efficient isolation of live microglia with preserved phenotypes from adult mouse brain. J Neuroinflammation. 2012; 9:147. [PubMed: 22742584]

Nimmerjahn A, Kirchhoff F, Helmchen F. Resting microglial cells are highly dynamic surveillants of brain parenchyma in vivo. Science. 2005; 308:1314–1318. [PubMed: 15831717]

Nimmerjahn F, Ravetch JV. Fcgamma receptors as regulators of immune responses. Nat Rev Immunol. 2008; 8:34–47. [PubMed: 18064051]

Papagno L, Almeida JR, Nemes E, et al. Cell permeabilization for the assessment of T lymphocyte polyfunctional capacity. Journal of immunological methods. 2007; 328:182–188. [PubMed: 17920073]

Pineau I, Lacroix S. Proinflammatory cytokine synthesis in the injured mouse spinal cord: multiphasic expression pattern and identification of the cell types involved. J Comp Neurol. 2007; 500:267–285. [PubMed: 17111361]

Pineau I, Sun L, Bastien D, Lacroix S. Astrocytes initiate inflammation in the injured mouse spinal cord by promoting the entry of neutrophils and inflammatory monocytes in an IL-1 receptor/MyD88-dependent fashion. Brain Behav Immun. 2010; 24:540–553. [PubMed: 19932745]

Ransohoff RM, Perry VH. Microglial physiology: unique stimuli, specialized responses. Annual review of immunology. 2009; 27:119–145.

Smith HS. Activated microglia in nociception. Pain Physician. 2010; 13:295–304. [PubMed: 20495595]

Stirling DP, Yong VW. Dynamics of the inflammatory response after murine spinal cord injury revealed by flow cytometry. J Neurosci Res. 2008; 86:1944–1958. [PubMed: 18438914]

Streit WJ. Microglia as neuroprotective, immunocompetent cells of the CNS. Glia. 2002; 40:133–139. [PubMed: 12379901]

Verdier M, Jayat C, Ratinaud MH, et al. Optimization of cell permeabilization for multiparametric flow cytometric analysis with lectin staining. Cytometry. 2000; 41:55–61. [PubMed: 10942897]

Walker PA, Bedi SS, Shah SK, et al. Intravenous multipotent adult progenitor cell therapy after traumatic brain injury: modulation of the resident microglia population. J Neuroinflammation. 2012; 9:228. [PubMed: 23020860]

Highlights

We used a controlled cortical impact mouse model for traumatic brain injury.

We immunomagnetically enriched brain cell suspensions for myeloid immune cells.

We stained surface antigens to identify microglia flow cytometrically as M1 or M2.

These methods allow quantitative measurement of microglial polarization states.

24 hours after TBI, microglial M1:M2 ratio increased in injured brain hemispheres.
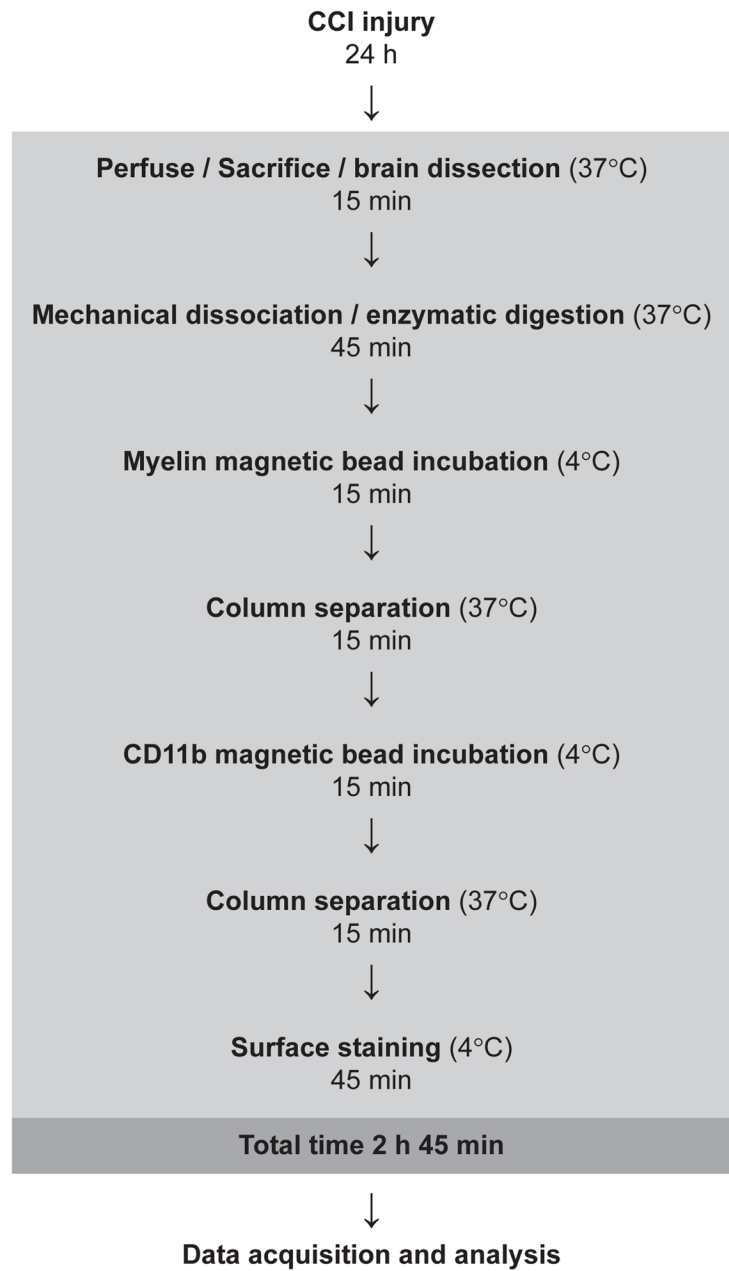
CCI injury
24 h
↓

Perfuse / Sacrifice / brain dissection (37°C)
15 min
↓

Mechanical dissociation / enzymatic digestion (37°C)
45 min
↓

Myelin magnetic bead incubation (4°C)
15 min
↓

Column separation (37°C)
15 min
↓

CD11b magnetic bead incubation (4°C)
15 min
↓

Column separation (37°C)
15 min
↓

Surface staining (4°C)
45 min

Total time 2 h 45 min

↓

Data acquisition and analysis

Fig. 1.
Sequence and timing of steps for preparation of injured mouse brain hemispheres for flow cytometry.
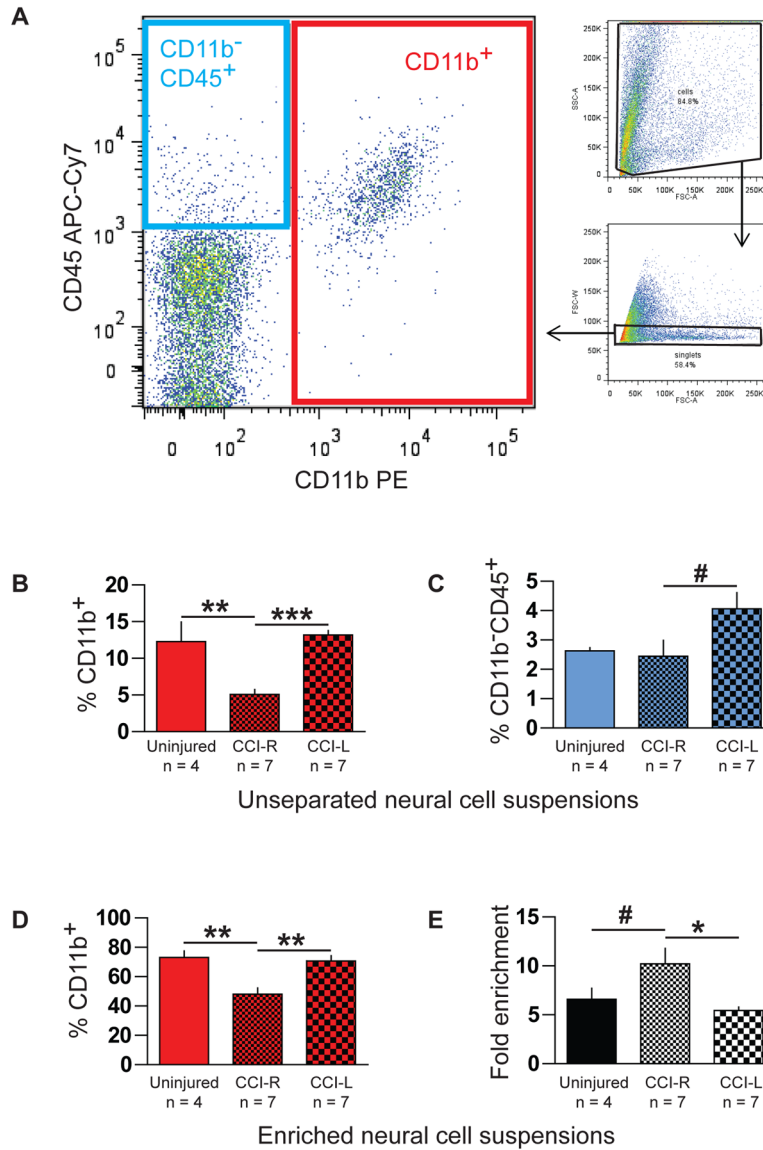
Fig. 2.
Percent myeloid and nonmyeloid leukocytes in unseparated and immunomagnetically enriched neural cell suspensions determined by flow cytometry. (A) CD11b$^+$ myeloid cells (large plot, red box) and CD11b$^-$CD45$^+$ nonmyeloid leukocytes (blue box) were enumerated after any remaining myelin debris and aggregates were eliminated by exclusion gates based on scatter characteristics (small plots). (B) Ipsilateral injured hemispheres (CCI-R) showed significantly lower pre-enrichment frequencies of CD11b$^+$ cells compared to contralateral hemispheres (CCI-L) and uninjured brains. (C) Increased frequencies of CD11b$^-$CD45$^+$ nonmyeloid leukocytes were observed in contralateral CCI-L versus ipsilateral CCI-R hemispheres. Purity (D) and fold enrichment (E) of CD11b-enriched cell suspensions also varied significantly in injured right hemispheres.
* indicates p <0.05, ** indicates p <0.01, *** indicates p <0.005, and # indicates one-tailed p ≤ 0.05

A

B

FSC-A   CD11b PE $F_c\gamma$RII/III PerCP-Cy5.5
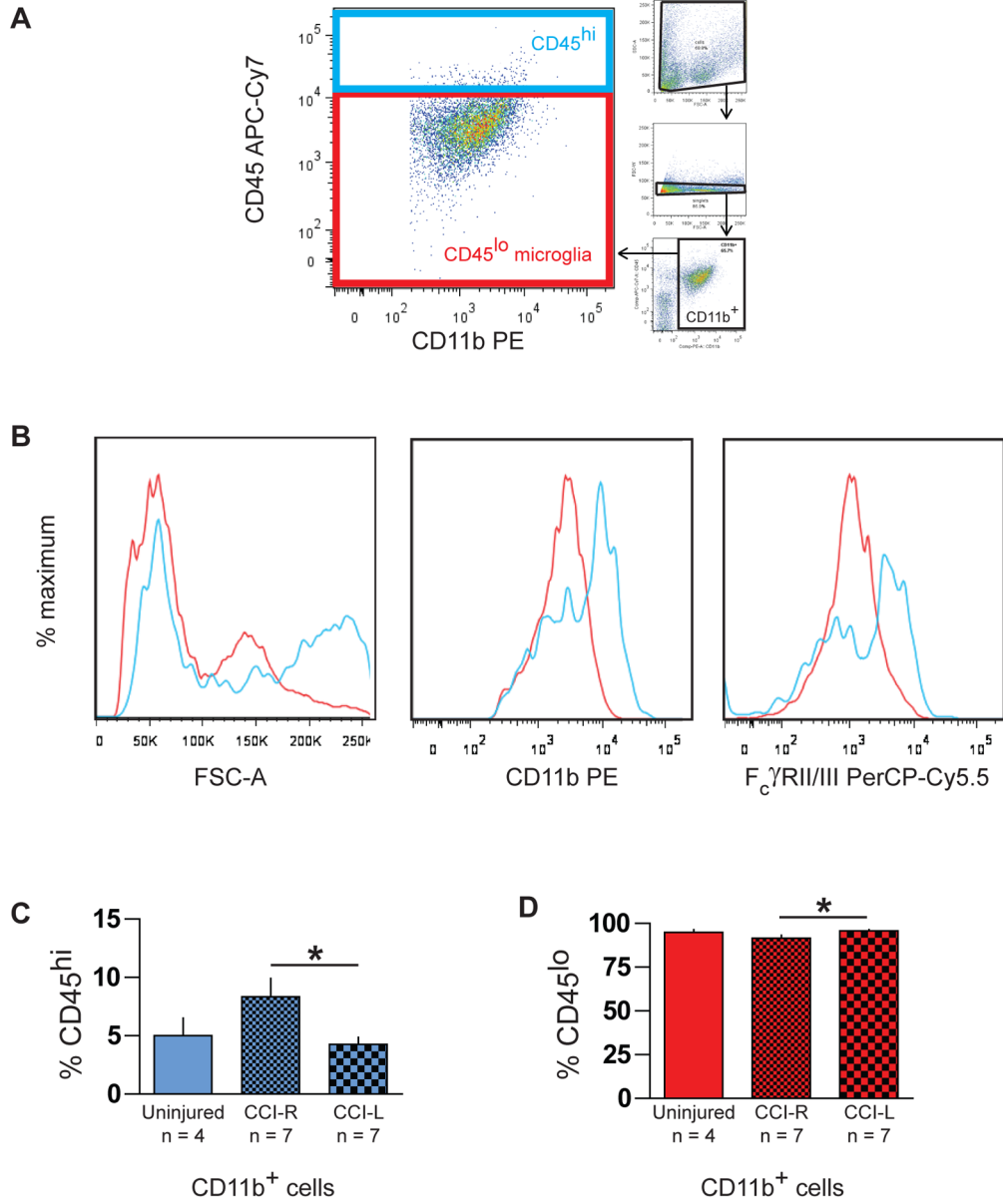
C

CD11b$^+$ cells

D

CD11b$^+$ cells

Fig. 3.
Two populations of CD11b$^+$ myeloid cells in immunomagnetically enriched neural cell suspensions identified by flow cytometry. (A) Both CD11b$^+$CD45^{lo} microglia (red box) and CD11b$^+$CD45^{hi} cells (blue box) were evident after excluding debris, aggregates, and CD11b$^-$ cells from the analysis (small plots). (B) Representative histograms display higher forward scatter (FSC-A) values and brighter CD11b and F_c RII/III staining of CD11b$^+$CD45^{hi} cells (blue lines) compared to the CD11b$^+$CD45^{lo} microglial population (red lines). (C, D) The relative frequencies of these two myeloid populations varied significantly between ipsilateral CCI-R and contralateral CCI-L hemispheres 24 hours after CCI injury.
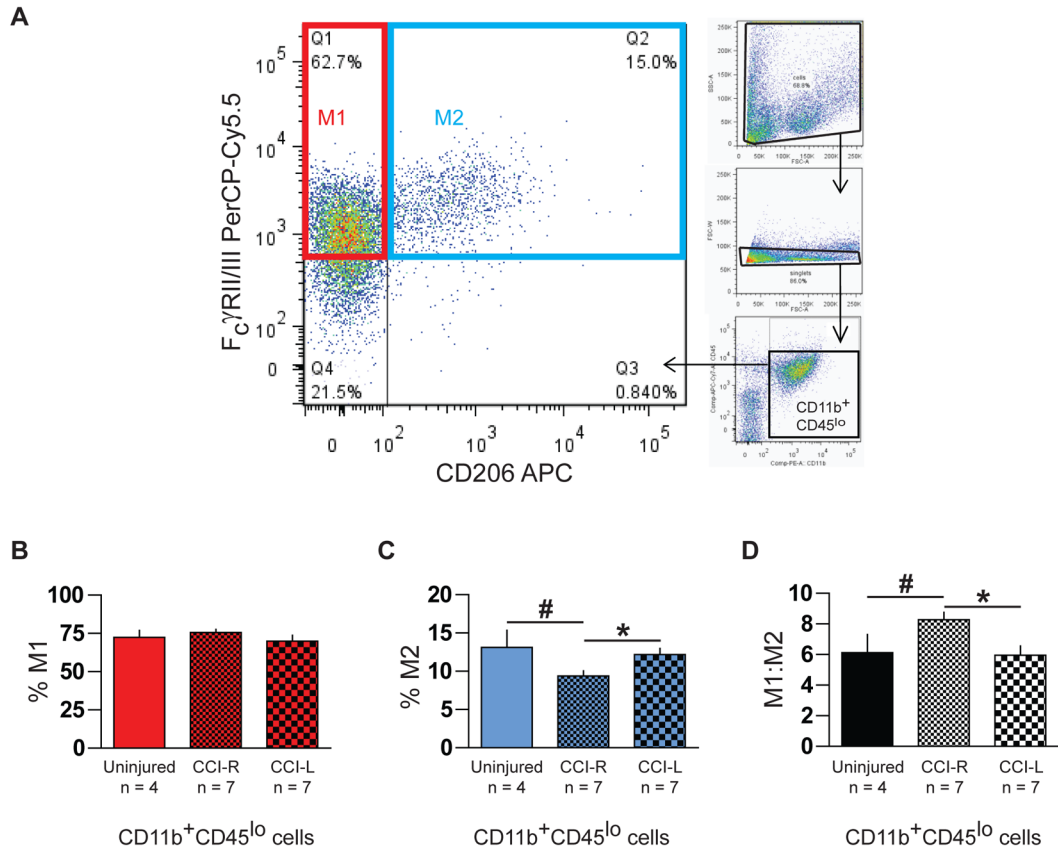* indicates p <0.05

Fig. 4.
M1 and M2 microglia in immunomagnetically enriched neural cell suspensions identified by flow cytometry. (A) CD11b^{+}CD45^{lo} microglia (large plot) were categorized as M1 (red box) or M2 (blue box) macrophage/microglia based on CD206 and F_c RII/III expression after excluding debris, aggregates, CD11b^{−}, and CD45^{hi} cells from the analysis (small plots). (B) Injured CCI-R hemispheres showed an increase in % M1 cells ($p = 0.0565$) compared to contralateral CCI-L hemispheres. (C) Injured CCI-R hemispheres also exhibited a significant decrease in % M2 cells compared to contralateral CCI-L hemispheres. (D) Correspondingly, the M1:M2 ratio, the number of M1 microglia divided by the number of M2 microglia, increased significantly in CCI-R compared to CCI-L hemispheres 24 hours after injury.

* indicates $p < 0.05$, # indicates one-tailed p 0.05